Proceedings of the Estonian Academy of Sciences,
2015, **64**, 3S, 438–448
doi: 10.3176/proc.2015.3S.15
Available online at www.eap.ee/proceedings

NONLINEAR WAVES

Wave nature in deformation of solids and comprehensive description of deformation dynamics

Sanichiro Yoshida

Department of Chemistry and Physics, Southeastern Louisiana University, Hammond, Louisiana 70402, USA; syoshida@selu.edu

Received 23 December 2014, accepted 16 July 2015, available online 28 August 2015

Abstract. Deformation of solids is discussed based on a recent field theory. Applying the basic physical principle, known as local symmetry, to the elastic force law, this theory derives field equations that govern dynamics of all stages of deformation on the same theoretical basis. The general solutions to the field equations are wave functions. Different stages of deformation are characterized by different restoring mechanisms that generate the wave characteristics. Elastic deformation is characterized by longitudinal restoring force, plastic deformation is characterized by transverse restoring force accompanied by longitudinal energy dissipative force. Fracture is characterized by the final stage of plastic deformation where the solid has lost both restoring and energy dissipative mechanisms. Experimental observations that support these wave dynamics are presented.

Key words: deformation of solids, plastic deformation transverse-wave, elasto-plastic solitary-wave.

1. INTRODUCTION

Conventionally, elastic deformation, plastic deformation and fracture of solids are discussed by different theories based on the phenomenology. In reality, elastic and plastic deformations coexist in a given stage; a freshly annealed metal specimen has a number of dislocations that are activated by an external load causing local plastic deformation, and a metal specimen about to fail recovers from the deformation to a certain extent if the load is removed. For accurate analysis of deformation and fracture, it is necessary to use a theory that can describe all stages of deformation comprehensively.

For comprehensive description of deformation and fracture, it is essential that the theory is based on a fundamental level of physics. In this regard, a recent field theory of deformation and fracture has strength [1]. Applying the physical principle known as local symmetry to the elastic force law (Hooke's law), this theory (the field theory) formulates all stages of deformation on the same theoretical basis. In the situation where elastic deformation coexists with plastic deformation, the regions experiencing elastic deformation (call the deformation structural element, DSE) obeys Hooke's law. Deformation dynamics in each DSE can be described by the deformation gradient tensor expressed in the local coordinate system (frame). When the applied load is low, the entire object is deformed approximately elastically as a single DSE. Mathematically, this means that the transformation representing the deformation gradient tensor (called transformation U) is coordinate-independent. When the solid enters the plastic regime (past the yield point), multiple DSE's start to behave differently from one another. Each DSE has its own principal axes along which it is stretched or compressed. Mathematically, the transformation U becomes coordinate-dependent. Components of the deformation tensor are first-order derivatives of the displacement. If the tensor is coordinate-dependent, it means that the displacement components have second or higher-order dependence on the space coordinates;

the force law becomes nonlinear when expressed in the global coordinates[1]. In other words, the linear elastic theory becomes not locally symmetric.

To regain the local symmetry, the field theory replaces the usual derivatives with covariant derivatives by adding a gauge term. This enables us to formulaically express the transformation U with the first-order derivatives in the global coordinate system, hence to describe deformation dynamics of the entire object with a single transformation. From the viewpoint of dynamics, since this formulaic description does not represent the true physics, some adjustment is necessary. The vector field derived from the gauge term, the gauge field, makes the adjustment via the field force acting on the charge of symmetry. In terms of the geometry, this adjustment can be viewed as that of the potential associated with the gauge field aligns all DSE's to the same orientation so that differential operation can be performed commonly in the global coordinate system. Hence, the potential is rotational by nature. Applying the Lagrangian formalism to the gauge field, the field theory derives field equations that describe the dynamics associated with the field force.

The solutions to the field equations are wave functions, reflecting the restoring nature of elasticity. The charge of symmetry is incorporated into the field equations as the source terms. The irreversibility of plastic deformation is represented by energy dissipative motion of the charge, which causes the plastic wave to decay. Fracture is formulated as the final stage of deformation where the material loses the mechanism to dissipate the mechanical energy provided by the external agent (the load). The aim of this paper is to discuss the deformation dynamics from the viewpoint of wave dynamics. It will be shown that elastic deformation is represented by longitudinal wave dynamics where the restoring force is longitudinal. Plastic deformation is represented by transverse wave dynamics where the restoring mechanism is shear force associated with the above-mentioned rotational potential and the longitudinal effect is energy dissipative being associated with the charge motion. A solitary wave can be generated in the transitional stage from the elastic to plastic regime. Supporting experimental observations will be discussed.

2. THEORETICAL

Details of the field theory can be found elsewhere [1]. In accordance with the above argument, the field theory defines covariant derivatives as $D_i = \partial/\partial x_i - \Gamma_i \equiv \partial_i - \Gamma_i$. Here Γ_i is the gauge term associated with the derivatives with respect to x_i. With this definition, the total differential of the i-th component of displacement vector ξ can be expressed as

$$D\xi_i = \left(\frac{\partial \xi_i}{\partial x} - \Gamma_x \xi_i\right) dx + \left(\frac{\partial \xi_i}{\partial y} - \Gamma_y \xi_i\right) dy + \left(\frac{\partial \xi_i}{\partial z} - \Gamma_z \xi_i\right) dz \equiv d\xi_i - A_i. \tag{1}$$

Here, A_i is the i-th component of the rotational vector that aligns all DSE's to regain the local symmetry of the linear elastic law. Figure 1 illustrates this situation schematically. In elastic deformation, the rotation matrix represents rigid body rotation of the material, which does not involve length change. In Eq. (1), the actual change in the length of displacement vector is all in $d\xi_i$. Thus, A_i can be identified as the i-th component of the rotation tensor (the asymmetric portion of the displacement gradient tensor) [2]. The temporal component of $\boldsymbol{A}$ can be understood as the same compensation effect in the time domain. In wave dynamics, the temporal differentiation of the wave function ψ is related to the spatial differentiation in the direction of the propagation vector $\boldsymbol{k}$ via phase velocity c as $\dot{\psi} = -(\nabla\psi)\cdot c\hat{k}$. This interpretation leads to the four-vector potential expression of $\boldsymbol{A}$ as

$$A^\mu = \left(A^0, A^1, A^2, A^3\right) = \left(\frac{\phi^0}{c}, A^1, A^2, A^3\right). \tag{2}$$

[1] Note that the coordinate dependence of the transformation matrix does not necessarily cause plastic deformation. Instead, it makes the deformation curvilinear. The deformation becomes plastic when the material exerts energy-dissipative longitudinal force, as will be discussed shortly. Also note that this nonlinearity is based on the coordinate dependence of the transformation matrix that represents linear elasticity as the base theory. Hence, the present field theory does not cover nonlinear elasticity in general unless we use a variable elastic modulus in the field equation.

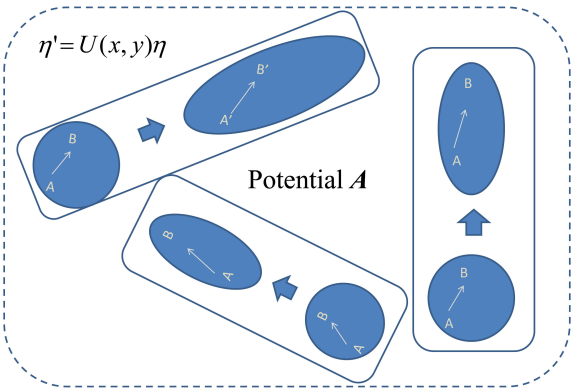

Fig. 1. Vector potential as displacement vector to align deformation structural elements. Transformation matrix U operating on a line element vector η changes its length.

The effect of $\boldsymbol{A}$ on the deformation dynamics at the global level can be formulated by comparing clockwise and counterclockwise covariant derivatives, or the quantity known as the field stress tensor $F_{\mu\nu}$:

$$F_{\mu\nu} \equiv \left[D_\mu, D_\nu\right] \xi_s ds = \left(\partial_\nu A_\mu - \partial_\mu A_\nu\right) + \frac{1}{\xi_s ds}\left[A_\mu, A_\nu\right]. \tag{3}$$

Each component of vector potential (2) represents a displacement. It is easily proved that they are commutable, hence $\left[A_\mu, A_\nu\right]$ term of Eq. (3) is zero. With this, we obtain the explicit form of $F_{\mu\nu}$ as

$$F_{\mu\nu} = \begin{pmatrix} 0 & -v^1/c & -v^2/c & -v^3/c \\ v^1/c & 0 & -\omega^3 & \omega^2 \\ v^2/c & \omega^3 & 0 & -\omega^1 \\ v^3/c & -\omega^2 & \omega^1 & 0 \end{pmatrix}. \tag{4}$$

Here $v^i,\ i = 1,2,3$ is the time derivative of A^i, and $\omega^i,\ i = 1,2,3$ is the rotation defined as

$$\omega^k = \frac{\partial A^j}{\partial x^i} - \frac{\partial A^i}{\partial x^j}, \tag{5}$$

c appearing in the time components of Eq. (4) is the phase velocity defined in Eq. (2). As $\boldsymbol{A}$ represents rotation of a DSE, we can identify c as representing the phase velocity due to the shear force that neighbouring deformation structural elements exert each other

$$c_{\text{shear}} = \sqrt{(G/\rho)}, \tag{6}$$

where G is the shear modulus and ρ is the density. It is easily proved that the trace $F_{\mu\nu}F^{\mu\nu}$ is invariant [2] under transformation U. This indicates that we can construct Lagrangian of the free particle (the dynamics of unit volume without the interaction with the gauge field or vector potential) in the form proportional to $F_{\mu\nu}F^{\mu\nu}$. Using the phase velocity (6) and adding the interaction terms with the gauge field, we can identify the full Lagrangian density as

$$L = -\frac{G}{4}F_{\mu\nu}F^{\mu\nu} + Gj^\mu A_\mu = \frac{\rho v^2}{2} - \frac{G\omega^2}{2} + \frac{G}{c}j^0 A_0 + Gj^i A_i. \tag{7}$$

Here the first two terms represent the Lagrangian density of the free particle in the form of the kinetic energy of the unit volume minus the rotational spring potential energy, and the third and fourth terms represent

the interaction; j^0 and j^i are the temporal and spatial components of the quantity known as the charge of symmetry, and they are connected with the phase velocity (6) as $j^\mu = (j^0/c, j^1, j^2, j^3)$. With Lagrangian density (7), the Euler-Lagrangian equation of motion associated with A_μ can be given as

$$\partial_\nu \frac{\partial L}{\partial(\partial_\nu A_\mu)} - \frac{\partial L}{\partial A_\mu} = 0. \tag{8}$$

This leads to the following field equations:

$$\nabla \cdot \boldsymbol{v} = -j_0, \tag{9}$$

$$\nabla \times \boldsymbol{v} = \frac{\partial \boldsymbol{\omega}}{\partial t}, \tag{10}$$

$$G\nabla \times \boldsymbol{\omega} = -\rho \frac{\partial \boldsymbol{v}}{\partial t} - G\boldsymbol{j}, \tag{11}$$

$$\nabla \cdot \boldsymbol{\omega} = 0. \tag{12}$$

Rearranging the terms, we can put the field equation (11) in the following form [2,3]:

$$\rho \frac{\partial \boldsymbol{v}}{\partial t} = -G\nabla \times \boldsymbol{\omega} - G\boldsymbol{j}. \tag{13}$$

The left-hand side of Eq. (13) is the product of the mass and acceleration of the unit volume. Hence, the right-hand side of Eq. (13) is the external force acting on the unit volume, where the first term $G\nabla \times \boldsymbol{\omega}$ is the shear force exerted by the neighbouring DSE's due to their differential rotations, and the second term $G\boldsymbol{j}$ is the longitudinal force density. The form of this second term differentiates the regimes of deformation from one another, as will be discussed below.

3. WAVE DYNAMICS OF DEFORMATION

3.1. Elastic compression wave

In the pure elastic regime, the field equations yield longitudinal wave solutions. By taking divergence of the left- and right-hand sides of Eq. (13) and using the mathematical identity $\nabla \cdot (\nabla \times \boldsymbol{\omega}) = 0$, we obtain

$$\rho \frac{\partial(\nabla \cdot \boldsymbol{v})}{\partial t} = -\nabla \cdot (G\boldsymbol{j}). \tag{14}$$

By putting $G\boldsymbol{j} = -(\lambda + 2G)\nabla(\nabla \cdot \xi)$ with the Lamé's constant λ, we can rewrite Eq. (14) as the following differential equation

$$\frac{\partial^2(\nabla \cdot \xi)}{\partial t^2} = \nabla^2 \frac{(\lambda + 2G)}{\rho}(\nabla \cdot \xi). \tag{15}$$

Here $\nabla(\nabla \cdot \xi)$ is the gradient of the volume expansion $\nabla \cdot \xi$ and $G\boldsymbol{j}$ represents the elastic force acting on a unit volume due to the differential stretch at the leading and tailing planes.

Equation (15) is the equation of elastic compression wave travelling at the phase velocity of $\sqrt{(\lambda + 2G)/\rho}$.

3.2. Plastic transverse decaying wave

In the pure plastic regime, the field equations yield transverse wave solutions reflecting the shear restoring force $G\nabla \times \boldsymbol{\omega}$ in Eq. (13). In Eq. (7), this force is associated with the rotational spring potential energy. In this case, the longitudinal force $G\boldsymbol{j}$ represents energy dissipative force as follows. Equation (14) can be viewed as the equation of continuity associated with the conservation of charge $\rho\nabla\cdot\boldsymbol{v} = -\rho j_0$ (called the deformation charge). Thus, we can put

$$G\boldsymbol{j} = \boldsymbol{W}_d\rho(\nabla\cdot\boldsymbol{v}), \tag{16}$$

where $\boldsymbol{W}_d$ is the drift velocity of the deformation charge of the unit volume. Optical interferometric fringe patterns[2] obtained in tensile experiments often show band patterns like the one shown at the top of Fig. 2 (enclosed by a dashed-line) [4–6]. As the middle drawing in this figure illustrates, the band pattern consists of concentrated, equi-distant, parallel fringes. As each fringe represents a contour of displacement, this pattern represents a quantity proportional to dv_i/dx_i where x_i is the coordinate axis the interferometer is sensitive to and v_i is the x_i-component of the velocity vector. When the interferometer is sensitive to a pair of orthogonal axes (the x and y axes), this type of pattern is observed at the same time and location in both axes [4]. Thus, it can be interpreted as representing $dv_s/dx_s = \partial v_i/\partial x_i + \partial v_j/\partial x_j = \nabla\cdot\boldsymbol{v}$, where s is the direction perpendicular to the parallel fringes and i and j are the orthogonal axes that the interferometer is sensitive to. Thus, this type of band-structured fringe pattern can be interpreted as a developed, one-dimensional deformation charge. Here the word "developed" is used to mean that the charge is across the

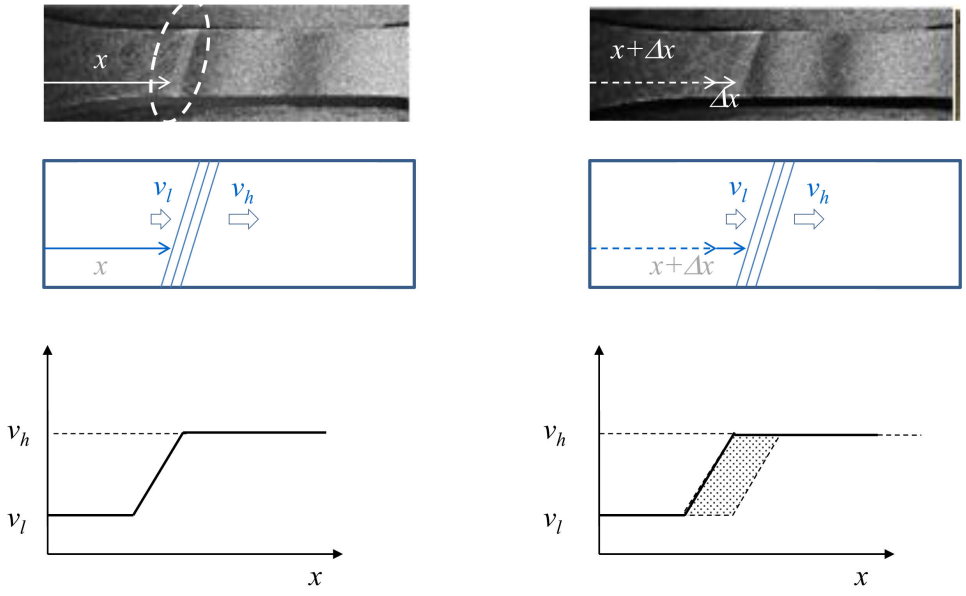

Fig. 2. Developed one-dimensional charge observed in a tensile experiment on a structural steel specimen with a constant cross-head speed of 2.5 (μm/s) [6].

[2] The fringe patterns are formed with the technique known as the Electronic Speckle-Pattern Interferometry (ESPI.) The ESPI setup takes the image of an object illuminated by a pair of laser beams originating from the same laser source at each time step while the object is being deformed. Each image consists of a number of speckles resulting from coherent superposition of the two laser beams, diffusively reflected off the object surface. The optical phase of each speckle is proportional to the relative optical path length of the two laser beams (beam 1 and beam 2.) When points of the object are displaced in such a way that the displacement increases the optical path length of beam 1 and decreases that of beam 2, the phase of the corresponding speckle changes accordingly. By subtracting the image taken at a certain time step from that taken in another time step, one can map out the pattern of the corresponding displacement as a two-dimensional fringe pattern. Here a dark fringe represents the contour of the displacement that corresponds to the phase change of an integer multiple of 2π.

width of the specimen, and the charge is considered to be one-dimensional as its spatial dependence can be expressed with the single variable x_s. The physical meaning of the developed charge can be argued as follows. When particles flow in x_s direction with a velocity gradient, the acceleration of a unit volume is $dv_s/dt = (dv_s/dx_s)(dx_s/dt) = (dv_s/dx_s)v_s$. Here $v_s = dx_s/dt$ is the average velocity of the particles in the unit volume. Thus, the external force that accelerates the unit volume is $\rho(dv_s/dt) = \rho(dv_s/dx_s)v_s = \rho(\nabla\cdot\boldsymbol{v})v_s$. Comparison of this acceleration and the right-hand side of Eq. (16) indicates that if $W_d = v_s$, $G\boldsymbol{j}$ is the external force that accelerates the unit volume. If $W_d > v_s$, as the bottom drawings of Fig. 2 indicate, the particles behind the band (the hatched portion in the drawing) experience reduction in their velocity, hence lose the momentum. It follows that if a positive/negative charge flows in the same/opposite direction to the local velocity of the material faster than the particles, the energy is dissipated via this mechanism of momentum loss. Here, a charge is said to be positive/negative when $\nabla\cdot\boldsymbol{v}$ is positive/negative. We can put

$$\boldsymbol{W}_d = \sigma_0\boldsymbol{v} \tag{17}$$

to express the degree of the energy dissipation; the greater is σ_0, the more energy is dissipated. The reduction in the particles' momenta behind a charge is due to reduction in the stiffness, caused by the propagation of dislocations. Dislocation theory explains that dislocations are driven by shear force and move at a constant velocity because the shear force is in equilibrium with frictional force [7]. The energy dissipative nature of the longitudinal force $G\boldsymbol{j}$ can be attributed to this frictional force. Since the frictional coefficient is a material constant, σ_0 can be considered as a material constant. In fact, a previous series of tensile experiments [8] on an aluminium alloy indicate that σ_0 is constant at approximately 3000 under different cross-head speeds in a range of 0.1 to 3.0 mm/min.

With Eqs (16) and (17), Eq. (13) becomes

$$\rho\frac{\partial\boldsymbol{v}}{\partial t} = -G\nabla\times\boldsymbol{\omega} - \sigma_0\rho(\nabla\cdot\boldsymbol{v})\boldsymbol{v} = -G\nabla\times\boldsymbol{\omega} - \sigma_c\boldsymbol{v}. \tag{18}$$

On the right-hand side, the first term is the recovery force due to shear deformation, and the second term represents the energy dissipation. Being proportional to the velocity, the second term can be interpreted as representing a velocity damping force, where $\sigma_c = \sigma_0\rho(\nabla\cdot\boldsymbol{v})$ is the damping coefficient. This effect is interpreted as the energy dissipative nature of plastic deformation. Elimination of $\boldsymbol{\omega}$ from Eq. (18) with the use of the field equation (10) leads to the following wave equation that governs $\boldsymbol{v}$:

$$\rho\frac{\partial^2\boldsymbol{v}}{\partial t^2} - G\nabla^2\boldsymbol{v} + \sigma_c\frac{\partial\boldsymbol{v}}{\partial t} = -G\nabla(\nabla\cdot\boldsymbol{v}). \tag{19}$$

Transverse wave characteristic has been experimentally observed in the displacement component perpendicular to the tensile axis in an aluminium alloy specimen under monotonic tensile load with the cross-head speed of 0.1 mm/min [9]. Figure 3 shows the oscillatory behaviour of the displacement, observed at a reference point P_2. In this experiment, a developed charge started to appear in the final stage of plastic deformation. The exponential decay of the oscillation observed prior to the appearance of the developed charge indicates that the charges are uniformly distributed over the specimen, allowing us to put $\nabla(\nabla\cdot\boldsymbol{v}) = 0$ on the right-hand side of Eq. (19). Under this condition, the general solution to Eq. (19) has the

$$\boldsymbol{v} = \boldsymbol{v}_0 e^{-\frac{\sigma_c}{2\rho}t}\cos\left(\left(\frac{G}{\rho}k^2 - \frac{\sigma_c^2}{4\rho^2}\right)^{1/2}t - \boldsymbol{k}\cdot\boldsymbol{r}\right). \tag{20}$$

Here $\boldsymbol{v}$ is the particle velocity vector, $\boldsymbol{v}_0$ is its amplitude, $\boldsymbol{k}$ is the propagation vector, and $\boldsymbol{r} = x\hat{x} + y\hat{y} + z\hat{z}$ is the position vector of the coordinate point. In the experiment that yields Fig. 3, the interferometer is sensitive to the x-component of $\boldsymbol{v}$ and the reference points P_1–P_3 (Fig. 3) are along a line of constant x, say x_0. The observed wave can then be put in the following form

$$v_x = v_{0x}e^{-\frac{\sigma_c}{2\rho}t}\cos\left(\left(\frac{G}{\rho}k^2 - \frac{\sigma_c^2}{4\rho^2}\right)^{1/2}t - k_y y + \phi_0\right). \tag{21}$$

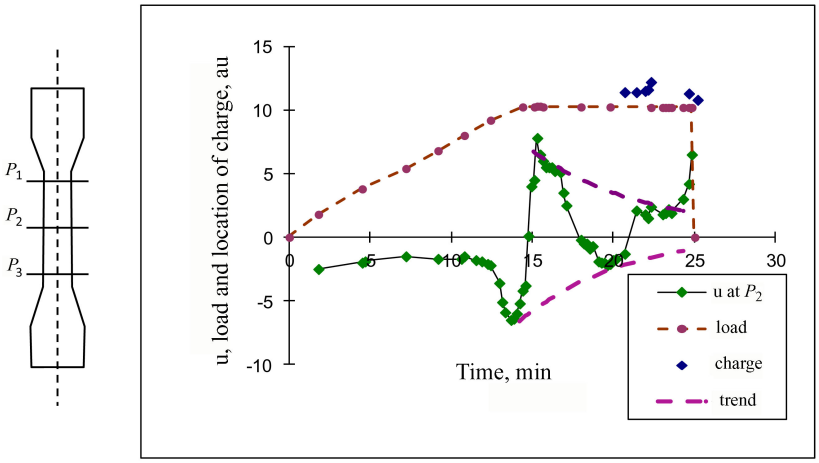

Fig. 3. Decaying oscillation observed in a transverse plastic deformation wave along with the loading characteristics. "u" is the velocity component perpendicular to the tensile axis. The dashed-line plot with circular markers shows the applied load. "charge" indicates the locations where developed charges appear. The dashed line is an exponential fit to the oscillation peaks.

Here x is the axis perpendicular to the tensile axis, v_x is the x-component of the velocity, v_{0x} is the amplitude, k_y is the y-component of the propagation vector, ϕ_0 is the constant phase associated with $-k_x x_0$ part of the phase term $\boldsymbol{k}\cdot\boldsymbol{r}$ in Eq. (20), and the z component is omitted as the ESPI setup does not have sensitivity in z. Equations (20) and (21) indicate that the time constant of the exponential decay is $2\rho/\sigma_c$:

$$\tau_c = \frac{2\rho}{\sigma_c} = \frac{2}{\sigma_0(\nabla\cdot\boldsymbol{v})}. \tag{22}$$

Based on the above hypothesis that σ_0 is a material constant and for aluminium alloys $\sigma_0 = 3000$, we can estimate the charge density $(\nabla\cdot\boldsymbol{v})$ for the case shown in Fig. 3. With $\tau_c = 400\ s$ as estimated from the exponential decay observed in this figure and Eq. (22), $(\nabla\cdot\boldsymbol{v}) = 2/(400\times 3000) = 1.7\times 10^{-6}\ (1/s)$. Note that this value of charge density is observed when the velocity field decays exponentially with no developed charge (like the one shown in Fig. 2) formed. It is interesting to compare this value with a typical value when a developed charge is formed. As mentioned above, the density of a developed charge can be expressed as $\nabla\cdot\boldsymbol{v} = dv_s/dx_s$ where s denotes the component perpendicular to the band structure of the charge. Considering that the tensile axis component of dv_s is approximately equal to the cross-head speed of 2.5×10^{-6} m/s (because under this condition the strain is concentrated within the region of the developed charge), and that the width of a typical band is 5 mm in the x_s direction and therefore 5.2 mm along the tensile axis[3], the charge density in this case can be evaluated as $dv_x/dx_s \cong 2.5\times 10^{-6}/5.2\times 10^{-3} = 4.8\times 10^{-4}\ (1/s)$. Apparently, the density of a developed charge is two-orders of magnitude higher than the above charge density estimated when a developed charge is not formed. Accordingly, the decay time constant is shorter by the same factor, being of the order of (s). This indicates that under the condition where a developed charge is formed, the wave characteristic of the velocity field decays instantaneously. This is consistent with a previous experimental observation [9] that the transverse wave characteristic disappears as a developed charge is formed.

Although this orders-of-magnitude increase in the charge density associated with the formation of a developed charge is a subject of future investigation, two factors can be argued as possible causes for the increase. The first factor is the transition of the longitudinal force from the purely elastic to plastic mode. The charge density $(\nabla\cdot\boldsymbol{v})$ is essentially the rate of the volume expansion $(\nabla\cdot\xi)$. When the dynamics is purely elastic, the volume expansion represents the local stretch and its rate is the elastic force represented

[3] The angle of the band to the tensile axis observed in Fig. 2 is used to calculate the band width along the tensile axis.

by the elastic longitudinal force $G\boldsymbol{j} = -(\lambda + 2G)\nabla(\nabla \cdot \xi)$, as discussed above. As the deformation develops towards the purely plastic regime, the longitudinal force becomes partially energy-dissipative as represented by $G\boldsymbol{j} = \boldsymbol{W}_d\rho(\nabla \cdot \boldsymbol{v})$. As this transition takes place, the effect of the shear restoring force $G\nabla \times \omega$ becomes substantial, generating the transverse wave characteristic in the velocity field. With further progress of deformation, the energy-dissipative portion of the volume expansion rate increases, contributing to the increase in the charge density $(\nabla \cdot \boldsymbol{v})$. The second factor is associated with the stress concentration. If the energy-dissipative volume expansion is uniformly distributed over the entire specimen, the energy dissipation takes place rather uniformly causing the exponential decay of the transverse wave as observed in Fig. 3. However, if for some reason, shear stress is intensified at a certain location of the specimen, the propagation of dislocations is enhanced locally and the shear strain is concentrated in that location. In other words, the volume expansion is localized, making the denominator of $(\nabla \cdot \boldsymbol{v}) = d\boldsymbol{v}_s/dx_s$ smaller even if the numerator $d\boldsymbol{v}_s$, the differential displacement at the boundaries (at the two grips of the tensile machine), remains the same. In this stage, it is expected that the damping coefficient $\sigma_c = \sigma_0\rho(\nabla \cdot \boldsymbol{v})$ is so high that the transverse wave characteristic cannot be sustained, as observed in Fig. 3 around $t = 21$ min when the first developed charge is formed.

3.3. Solitary wave in transitional regime

Experiments [4–6] show that in the transitional stage from the elastic to the plastic regime, a deformation charge similar to Fig. 3 drifts continuously. From various behaviours such as that the drift velocity is proportional to the tensile (cross-head) speed, this type of deformation charge has been identified as representing the same physical event as the Lüders band [6]. As shown in Fig. 2, inside a deformation charge of this type the velocity field depends only on x_s, the coordinate axis perpendicular to the parallel fringes; i.e., $\partial/\partial x_p = 0$ in the two-dimensional picture, where x_p is the axis parallel to the fringes. This situation leads to $(\nabla \times \omega)_s = 0$, and $\nabla \cdot \boldsymbol{v} = dv_s/dx_s$. The former condition indicates that in the direction perpendicular to the fringes (the band), the shear force is ineffective. The latter condition indicates that the longitudinal force in this direction can be either the elastic force proportional to $d\xi_s/dx_s$, the energy-dissipative force proportional to dv_s/dx_s, or both. Here, we continue the argument assuming that both types of longitudinal force are effective. Since $\partial/\partial x_p = 0$, the Poisson's effect is inactive in the elastic deformation, and the dynamics along the x_s axis can be treated as a one-dimensional problem similar to a longitudinal compression wave propagating through a bar of elastoviscous medium. Judging from the fringe pattern that exhibits null or very little deformation outside the banded region, we can assume that this elastoviscous dynamics is localized in the banded region. Considering that the displacement of the banded region (the charge) from its equilibrium position, X, is the differential displacement of its front and back end, we can express the potential energy of the region due to elasticity as

$$U = \frac{1}{2}k_s X^2 = \frac{1}{2}k_s\left(\frac{\partial^2\xi_s}{\partial x_s^2}\right)^2(\delta x_s \Delta x_s)^2 = \frac{SE}{2}\left(\frac{\partial^2\xi_s}{\partial x_s^2}\right)^2 \delta x_s(\Delta x_s)^2, \tag{23}$$

where k_s is the spring constant (stiffness) in the x_s direction, S is the cross-sectional area, E is the Young's modulus, δx_s is the infinitesimal width of the front and back ends of the band, and Δx_s is the width (span) of the band. This leads to the Lagrangian density as

$$L_{\text{charge}} = \frac{U}{S\Delta x_s} = \frac{E}{2}\left(\frac{\partial^2\xi_s}{\partial x_s^2}\right)^2(\delta x_s \Delta x_s) = \frac{E}{2}(\partial_{x_s}^2\xi_s)^2(\delta x_s \Delta x_s), \tag{24}$$

and the corresponding term of the Euler Lagrangian equation of motion as

$$\partial_{x_s}^2\left(\frac{\partial L_{\text{charge}}}{\partial(\partial_{x_s}^2\xi)}\right) = E\partial_{x_s}^2(\partial_{x_s}^2\xi_s)(\delta x_s \Delta x_s) = E\partial_{x_s}^4\xi_s(\delta x_s \Delta x_s) = -\frac{E}{c_w}\partial_{x_s}^3(\partial_t\xi_s)(\delta x_s \Delta x_s). \tag{25}$$

Here the spatial derivative is replaced with the temporal derivative as $\partial_{x_s}\xi_s = -\partial_t\xi_s/c_w$ (the same replacement as Eq. (2) where c_w is the phase velocity in this case) going through the last equal sign. Equation (25) represents the elastic force acting on the charge. With this force, Eq. (18) becomes

$$\rho\partial_t v_s = -\sigma_0 v_s \rho \partial^1_{x_s} v_s - \frac{E\delta x_s \Delta x_s}{c_w}\partial^3_{x_s} v_s, \tag{26}$$

where $\nabla\cdot\boldsymbol{v}$ is replaced by $\partial^1_{x_s} v_s \equiv \partial v_s/\partial x_s$. Equation (26) is known to yield solitary-wave solutions in the following form [10].

$$v_s = a\, sech^2\left(b(x_s - c_w t)\right). \tag{27}$$

Here a is the amplitude in (m/s), b is a shape constant in $(1/\mathrm{m})$, and c_w is the wave velocity in (m/s). Substitution of Eq. (27) into Eq. (26) leads to the following conditions for c_w and b:

$$c_w = \frac{\sigma_0 a}{3}, \tag{28}$$

$$b = \left(\frac{\sigma_0 a}{3}\right)\sqrt{\frac{\rho}{4E\delta x_s \Delta x_s}}. \tag{29}$$

Condition (28) indicates that the solitary wave velocity c_w is proportional to the particle velocity at the peak of the solitary wave (the amplitude a in Eq. (27).) Since the particle velocity is proportional to the cross-head speed, this is consistent with the experimental observation that the drift velocity of a Lüders band is proportional to the tensile speed.

Interpreting that the solitary wave causes energy dissipation by the mechanism discussed in Fig. 2, we can put $c_w = W_d$. From Eq. (17), this leads to $a = 3v$, where v is the nominal particle velocity (the velocity that the particle would have if the charge did not flow), indicating that the peak particle velocity in a solitary wave is three times higher than the nominal particle velocity. The observation that at the peak of the solitary wave the particle moves faster than the nominal velocity leads to the following argument, which connects the solitary wave dynamics to the conventional, microscopic-deformation dynamics. Dislocation theory explains that dynamic dislocations propagate in the direction of the maximum shear stress and that a Lüders band is formed when the dislocations complete their propagation across the width of a specimen, bridging the two sides of the specimen. When this bridging event takes place, the material slips along the line of the maximum shear stress. This reconfigures the local atomic arrangement, causing a partial breakage of the material. A previous experimental observation that the formation of the optical band pattern representing a developed charge is accompanied by acoustic emission [11] supports this argument. As this partial breakage occurs, the material recoils in mutually opposite directions on the two sides of the partial breakage (both sides shrink back in the respective directions). Near the centre of this region, it is expected that the recoiling velocity exceeds the nominal particle velocity determined by the cross-head speed.

Solitary waves are known to retain their shapes while interacting with one another. No experimental observation has been made that demonstrates multiple, developed charges or Lüders bands passing one another. Whether or not the present type of solitary waves retain their shapes on interaction is an interesting subject for future investigation, and some comments are being made here. In tensile experiments with a constant cross-head speed, often a pair of developed charges generated near the two ends of a specimen (near the shoulder at each end where the width of the dog-bone style specimen increases from that of the middle parallel part to the wider part gripped by the tensile machine) are observed to move toward the middle of the specimen at the same speed, and disappear as soon as they run into each other. It seems that this phenomenon represents the fact that once Lüders bands complete sweeping the entire specimen the mechanism that sustains the dislocations to keep bridging the specimen at the front of the band ceases, and therefore a new band is not formed anymore. It is unlikely that it represents that the two solitary waves destroy each other. It is well known that in the case of carbon steels Lüders bands sweep along the specimen

only once during the yield plateau, and that as soon as the sweep is over the stress resumes to rise[4]. From the viewpoint of microscopic deformation, the following argument indicates that developed charges retain their shapes, if they pass each other. According to dislocation theory, dislocations associated with Lüders bands propagate along the line of maximum shear stress, not on a specific crystallographic plane. Therefore, it is impossible for the dislocations of one charge to switch their path onto that of the other interacting charge (cross-slipping does not occur).

Noting that $\sqrt{E/\rho}$ represents the phase velocity of a longitudinal elastic wave c_{elas}, we can rewrite Eq. (29) in the following form

$$b = \frac{c_w}{c_{\text{elas}}} \frac{1}{4\sqrt{\delta x_s}\sqrt{\Delta x_s}}. \tag{30}$$

With typical values of $c_{\text{elas}} = 5.2$ km/s, $c_w = 100$ mm/min and $b^{-1} = 5$ mm (the inverse of a width of developed band-like charge), Eq. (30) leads to $\sqrt{\delta x_s}\sqrt{\Delta x_s} = 4 \times 10^{-10}$ m. In the infinitesimal limit, $\delta x_s = \Delta x_s$. Thus, this estimation leads to $\delta x_s = \Delta x_s$ of the order of a few angstrom. This value is comparable to the inter-atomic distance. This observation indicates that the elastic dynamics within a developed change occurs at the atomistic scale.

4. CONCLUSIONS

Wave dynamics of deformation have been discussed based on a recent field theory. The field equations have been derived with the use of the Lagrangian formalism. It has been shown that the field equations represent the spatiotemporal behaviour of the differential displacement field of the object under deformation. Longitudinal wave characteristics in the pure elastic regime, transverse, decaying wave characteristics in the pure plastic regime, and solitary wave characteristics in the transitional stage from the elastic to plastic regime have been derived as solutions to the field equations, and their physical meanings have been discussed. Some experimental observations that exhibit these wave dynamics have been presented. Further investigations are necessary to consolidate the theorization of these wave dynamics, in particular, the solitary wave dynamics.

REFERENCES

1. Yoshida, S. *Deformation and Fracture of Solid-State Materials.* Springer, New York, Heidelberg, London, 2015.
2. Yoshida, S. Scale-independent approach to deformation and fracture of solid-state materials. *J. Strain Anal.*, 2011, **46**, 380–388.
3. Yoshida, S. Dynamics of plastic deformation based on restoring and energy dissipative mechanism in plasticity. *Phys. Mesomech.*, 2008, **11**(3–4), 140–146.
4. Yoshida, S., Widiastuti, R., Pardede, M., Hutagalung, S., Marpaung, J. S., Muhardy, A. F., and Kusnowo, A. Direct observation of developed plastic deformation and its application to nondestructive testing. *Jpn. J. Appl. Phys.*, 1996, **35**, L854–L857.
5. Yoshida, S. and Toyooka, S. Field theoretical interpretation of dynamics of plastic deformation – Portevin-Le Chatelie effect and propagation of shear band. *J. Phys. Condens. Matter*, 2001, **13**(31), 6741–6757.
6. Yoshida, S., Ishii, H., Ichinose, K., Gomi K., and Taniuchi, K. An optical interferometric band of an indicator of plastic deformation front. *J. Appl. Mech.*, 2005, **72**(5), 792–794.
7. Suzuki, T., Takeuchi, S., and Yoshinaga, H. *Dislocation Dynamics and Plasticity*. Springer, Berlin, New York, Tokyo, 1991.
8. Yoshida, S. and Sasaki, T. Field theoretical description of shear bands. *Soc. Exp. Mech. Annual Meeting*, June 8–11, 2015, Costa Mesa, CA, USA.

[4] In other materials such as aluminium alloys, sometimes developed charge similar to Fig. 2 are observed to sweep along the specimen a number of times. The appearance of this type of charges is not exactly continuous; rather it is intermittent with a short interval. The stress resumes to rise after each relaxation associated with the appearance of this type of charge. The next charge appears at a different location as the location of the maximum shear stress moves along with the rotational (ω) wave travels. Here the rotational wave is given as a solution to the field equations (9)–(12), and the line of the maximum shear stress runs along the boundary of a pair of unlike rotations (ω of mutually opposite signs.) The fourth field equation (12) assures that unlike rotations always pair.

9. Yoshida, S., Siahaan, B., Pardede, M. H., Sijabat, N., Simangunsong, H., Simbolon, T., and Kusnowo, A. Observation of plastic deformation wave in a tensile-loaded aluminum-alloy. *Phys. Lett. A.*, 1999, **251**(1), 54–60.
10. Maugin, G. A. Solitons in elastic solids (1938–2010). *Mech. Res. Commun.*, 2011, **38**(5), 341–349.
11. Yoshida, S. Optical interferometric study on deformation and fracture based on physical mesomechanics. *Phys. Mesomech.*, 1999, **2**(4), 5–12.

Tahkiste deformatsiooni lainelaadne iseloom ja deformatsioonidünaamika üksikasjalik kirjeldus

Sanichiro Yoshida

On uuritud tahkiste deformatsiooni, lähtudes tänapäevasest väljateooriast. Lagrange'i formalismist lähtudes on tuletatud väljavõrrandid, mis kirjeldavad kõiki deformatsioonistaadiume samadel teoreetilistel alustel. Väljavõrrandite üldlahenditeks on lainefunktsioonid. Erinevatele deformatsioonistaadiumidele on iseloomulikud erinevad taastumismehhanismid: elastset deformatsiooni iseloomustab taastav pikijõud, plastset deformatsiooni aga taastav põikjõud koos energia dissipatsioonist põhjustatud pikijõuga. Purunemist vaadeldakse kui plastse deformatsiooni viimast staadiumi, kus tahkises on kadunud nii taastumis- kui ka dissipatsioonimehhanismid. Artiklis on esitatud ka teoreetilisi arutlusi kinnitavaid eksperimentaalseid tulemusi.